Amirkabir University of Technology
(Tehran Polytechnic)
Vol. 48, No. 1, Spring 2016, pp. 1- 10

Amirkabir International Journal of Science& Research
(Modeling, Identification, Simulation & Control)
(AIJ-MISC)

Supervisory Control of a Hybrid AC/DC Micro-Grid with Load Shedding Based on the Bankruptcy Problem

M. Hosseinzadeh[1] and F. Rajaei Salmasi[2*]

1-Ph.D Student, School of Electrical and Computer Engineering, University of Tehran, Tehran, Iran
2-Associate Professor, School of Electrical and Computer Engineering, University of Tehran, Tehran, Iran

Received 21 September 2015, Accepted 30 January, 2016

ABSTRACT

In this paper, a supervisory controller is proposed to manage the power flow in a hybrid AC/DC micro-grid for both grid-connected and disconnected modes. When the hybrid AC/DC micro-grid is connected to the utility grid, power surplus or shortage leads to the power trade between the micro-grid and the utility grid. In the grid-disconnected mode, the renewable power sources (wind and solar generation subsystems) are responsible of supplying the power demanded by the loads by themselves. In this case, the loads are classified as critical and non-critical loads, where critical loads are those that should be supplied in any condition. When the maximum available power is smaller than the power demanded by the critical loads, the battery banks are set in the discharging mode to satisfy the demand. Otherwise, the non-critical loads are supplied according to the proposed load shedding scheme, which is developed based on the bankruptcy problem. In summary, this paper proposes a new supervisory controller for a hybrid AC/DC micro-grid as well as a new load shedding scheme to supply the non-critical load in grid-disconnected mode. The effectiveness of the proposed supervisor controller is evaluated through simulation.

KEYWORDS

Hybrid AC/DC Micro-Grid, Power Management, Wind Turbine System, Photovoltaic Array System, Load Shedding, Bankruptcy Problem.

*Corresponding Author, Email: frajaei@ut.ac.ir

1. INTRODUCTION

A hybrid AC/DC micro-grid is introduced as a favorable solution to the problems of existing AC distribution systems coupling DC sources with DC loads and AC sources with AC loads [1]. A typical hybrid AC/DC micro-grid configuration, which is also used in this paper, is shown in Fig. 1, where Photovoltaic array and wind turbine are used as DC and AC power generation systems, respectively. Also, two separate battery banks are connected to AC and DC micro-grids in order to storage energy. It is worth noting that the loads are also classified as critical and non-critical loads, where the critical loads are the ones which should be supplied in any condition.

The hybrid AC/DC micro-grid can be either connected to the utility grid or disconnected from it [2]. When the hybrid AC/DC micro-grid is connected to the utility grid, the generation systems are forced to produce their maximum capacity. In this case, the main converter injects possible power surpluses to the utility grid. Also, possible power shortages are supplied by the utility grid. When the utility grid is disconnected from the hybrid AC/DC micro-grid, the generation systems are responsible to supply the demanded power by themselves.

In order to use the hybrid AC/DC micro-grid to maximum advantage, a supervisory controller is needed to manage the power split between different generation systems as well as power flow between AC and DC micro-grids. Most of the presented supervisory controllers in literature are designed to manage the power flow in a DC micro-grid for both grid-connected and disconnected operating modes [3]-[10].Regarding the power management issue in the hybrid AC/DC micro-grids, few works are reported in the literature. In [11], a hybrid AC/DC micro-grid consisting a wind generator as an AC source and a PV array as a DC source is presented, where a supervisory controller is proposed to manage the power flow in the hybrid AC/DC micro-grid. In [12]-[14], a droop-based controller is introduced to manage power sharing between the AC and DC micro-grids. In this paper, the AC and DC micro-grids are treated as two separate entities with individual droop representations, where the information from these two droop characteristics are merged to decide the amount of power to be exchanged between the micro-grids. In [15] and [16], only the amount of power which should be exchanged between the micro-grids are determined through a supervisory controller. A supervisory controller for a hybrid AC/DC micro-grid is presented in [17] by its authors.

On the other hand, in the presented works, it is assumed that the maximum available power is always more than the total power demand, and when the micro-grid is disconnected from the utility grid, the generation systems are enforced to supply the whole power demand. It is noteworthy that although power generation systems are installed, considering the total amount of loads in the disconnected operation mode, changing in weather condition may lead to power shortage in the micro-grid. Therefore, in practice, some amount of load must almost

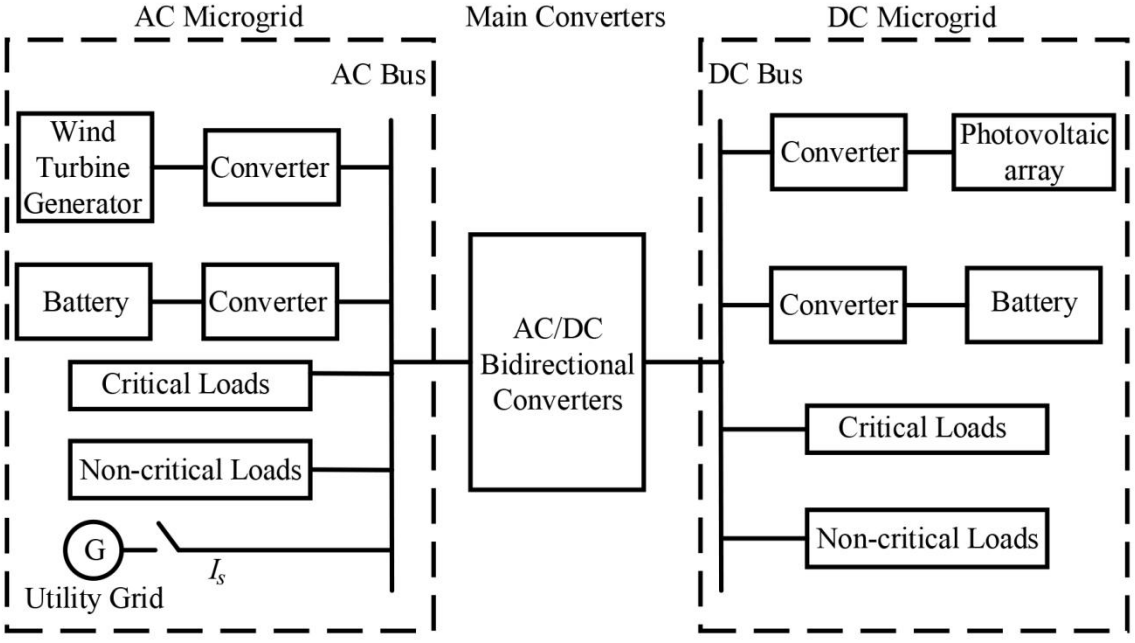

Fig. 1. **A typical hybrid AC/DC micro-grid configuration**

be instantly removed from a power system to keep the remaining portion of the system operational; this procedure is called load shedding.

In this paper, a supervisory controller for a hybrid AC/DC micro-grid is proposed to manage the power flow between the AC and DC micro-grids, as well as power split between the solar and wind generation systems. When the hybrid AC/DC micro-grid is connected to the utility grid, the possible power imbalances are solved through power exchange with the utility grid. When the hybrid AC/DC micro-grid operates in the grid-disconnected operating mode and there is power surplus, the supervisory controller injects the extra power to the battery banks and charges them. When the hybrid AC/DC micro-grid operates in the grid-disconnected operating mode and there is power shortage, two conditions may happen: (1) maximum available solar and wind power is less than the power demanded by the critical loads, and (2) maximum available solar and wind power is more than the power demanded by the critical loads. In the first case, the supervisory controller sends the discharge command to battery banks to supply the power shortage. In the latter case, a load shedding scheme will be proposed in this paper to reduce the amount of non-critical load intentionally.

The remainder of this paper is organized as follows. Sections II and III give a brief overview of the renewable power source models and their corresponding converters, where the models of wind turbine as the source of the AC micro-grid is given in Section II, and the model of PV panel as the source of the DC micro-grid is given in Section III. The bankruptcy problem and the proposed load shedding scheme is presented in Section IV. In Section V, a supervisory controller is proposed to manage the power flow in the hybrid AC/DC micro-grid. The simulation results obtained with the proposed supervisory controller are also reported in Section VI. Finally, the conclusion section summarizes the main outcome of this paper.

2. AC MICRO-GRID MODELING

The topology of the AC micro-grid under consideration in this paper is depicted in Fig. 2. The wind generation system is constituted by a windmill, a multipolar permanent magnet synchronous generator (PMSG), a rectifier, and a DC/DC converter. It should be remarked that the power generated by the wind turbine is controlled through the corresponding DC/DC converter. The mechanical output power of the turbine expressed in W can be calculated by the following equation:

$$P_m = \frac{1}{2} C_p(\lambda) \rho A v_{wind}^3 \quad (1)$$

where ρ is air density expressed in Kg/m^3, v_{wind} is wind speed expressed in m/s, and A is turbine swept area expressed in m^2. Also $\lambda = r\omega_m / v_{wind}$, where r is the blade length, and ω_m is angular shaft speed. It is worth noting that $C_p(\lambda)$ is performance coefficient of the turbine and is modeled as follows:

$$C_p(\lambda) = C_1 \left(\frac{C_2}{\lambda_i} - C_3\right) e^{-\frac{C_4}{\lambda_i}} + C_5 \lambda \quad (2)$$

where $\frac{1}{\lambda_i} = \frac{1}{\lambda} - 0.035$, $C_1 = 0.5176$, $C_2 = 116$, $C_3 = 5$, $C_4 = 21$, $C_5 = 0.0068$ [18]. Also, the wind turbine torque is given by

$$T_t = \frac{p_m}{\omega_m} = \frac{1}{2} C_t(\lambda) \rho A r v_{wind}^2 \quad (3)$$

where $C_t(\lambda) = C_p(\lambda)/\lambda$ is torque coefficient of the turbine.

As shown in Fig. 2, the wind turbine is linked with a PMSG, whose dynamic model in a rotor reference frame is given by the following equations [19]:

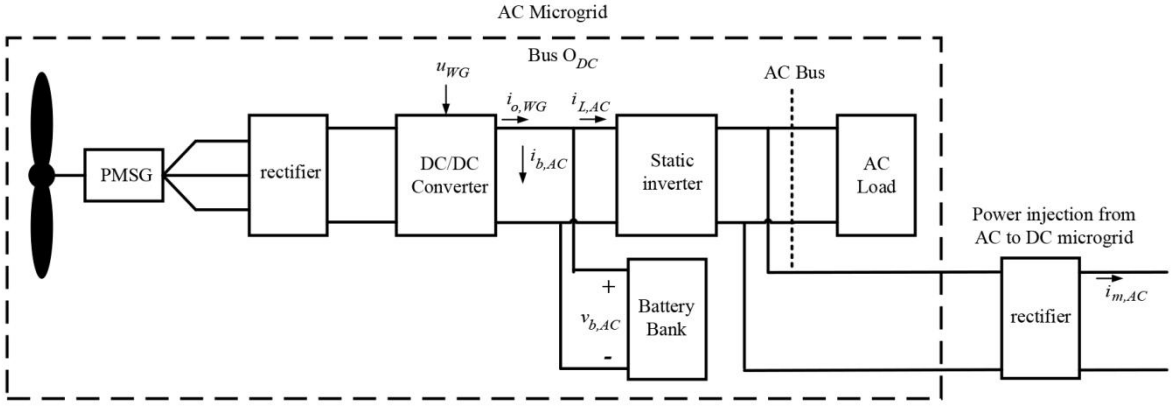

Fig. 2. AC micro-grid scheme

$$\begin{cases} \frac{di_q}{dt} = -\frac{R_s}{L_q} i_q - \omega_e i_d + \frac{\omega_e \phi_m}{L_q} - \frac{v_q}{L_q} \\ \frac{di_d}{dt} = -\frac{R_s}{L_d} i_d - \omega_e i_q - \frac{v_d}{L_d} \end{cases} \quad (4)$$

Where (v_d, v_q), (i_d, i_q) and (L_d, L_q) are terminal voltages, currents and stator inductances in the d-q axes, respectively, $\omega_e = \frac{P}{2}\omega_m$ is electrical angular speed with P denoting the number of poles, and ϕ_m is the flux linked by the stator windings. Note that in actual radial flux PMSGs with a smooth air-gap, $L_q \cong L_d = L$ holds. The terminal voltages (v_d, v_q) can be written as:

$$v_d = \frac{\pi v_{b,AC} i_d}{3\sqrt{3}\sqrt{i_d^2+i_q^2}} u_{WG}, \; v_q = \frac{\pi v_{b,AC} i_q}{3\sqrt{3}\sqrt{i_d^2+i_q^2}} u_{WG} \quad (5)$$

where $v_{b,AC}$ is the voltage of the bus O_{DC}, and $u_{WG} = k_{tr}/\delta$ in which k_{tr} is the winding ratio of the transformer included in the DC/DC converter, where δ is the DC/DC converter duty cycle.

Thus, Equation (4) can be rewritten as (6):

$$\begin{cases} \frac{di_q}{dt} = -\frac{R_s}{L} i_q - \omega_e i_d + \frac{\omega_e \phi_m}{L} - \frac{\pi v_{b,AC} i_d}{3\sqrt{3}L\sqrt{i_d^2+i_q^2}} u_{WG} \\ \frac{di_d}{dt} = -\frac{R_s}{L} i_d - \omega_e i_q - \frac{\pi v_{b,AC} i_q}{3\sqrt{3}L\sqrt{i_d^2+i_q^2}} u_{WG} \end{cases} \quad (6)$$

The electrical load torque produced by the PMSG can also be calculated as:

$$T_e = \frac{3}{2}\frac{P}{2}\phi_m i_q \quad (7)$$

Besides, assuming an ideal static conversion, the output current of the DC/DC converter is

$$i_{o,WG} = \frac{\pi}{2\sqrt{3}}\sqrt{i_q^2 + i_d^2}\, u_{WG} \quad (8)$$

The bus O_{DC} delivers the energy generated by the wind generator to the AC load, and if necessary, to the battery bank. Also, its voltage is imposed by the battery bank. Here, the lead-acid battery bank is modeled as a voltage source $E_{b,AC}$ connected in series with a resistance $R_{b,AC}$ and a capacitance $C_{b,AC}$. Thus, the bus O_{DC} voltage $(v_{b,AC})$ can be written by

$$v_{b,AC} = E_{b,AC} + v_{c,AC} + \left(\frac{\pi}{2\sqrt{3}}\sqrt{i_d^2 + i_q^2}\, u_{WG} - i_{L,AC}\right) R_{b,AC} \quad (9)$$

where $v_{c,AC}$ is the voltage in the capacitor $C_{b,AC}$. Also, assuming an ideal inverter, the AC load current can be referred to the bus O_{DC} as an output variable current $i_{L,AC}$.

Finally, supposing J as the inertia of the rotating system, the whole dynamic model of the AC micro-grid will be as given in (10), shown at the foot of the page. It is worth noting that, the current $i_{m,AC}$ presented in Fig. 2 corresponds to the power injected from the AC micro-grid to the DC one.

$$\begin{cases} \frac{di_q}{dt} = -\frac{R_s}{L} i_q - \omega_e i_d + \frac{\omega_e \phi_m}{L} - \frac{\pi v_{b,AC} i_d}{3\sqrt{3}L\sqrt{i_d^2+i_q^2}} u_{WG} \\ \frac{di_d}{dt} = -\frac{R_s}{L} i_d - \omega_e i_q - \frac{\pi v_{b,AC} i_q}{3\sqrt{3}L\sqrt{i_d^2+i_q^2}} u_{WG} \\ \frac{d\omega_e}{dt} = \frac{P}{2J}\left(T_t - \frac{3}{2}\frac{P}{2}\phi_m i_q\right) \\ \frac{dv_{c,AC}}{dt} = \frac{1}{C_{b,AC}}\left(\frac{\pi}{2\sqrt{3}}\sqrt{i_d^2 + i_q^2}\, u_{WG} - i_{L,AC}\right) \end{cases} \quad (10)$$

3. DC MICRO-GRID MODELING

The DC micro-grid, as shown in Fig. 3, comprises PV array connected to the DC bus via a DC/DC converter, which controls the operation point of the PV array. The PV array generated current is calculated through the following equation [20]:

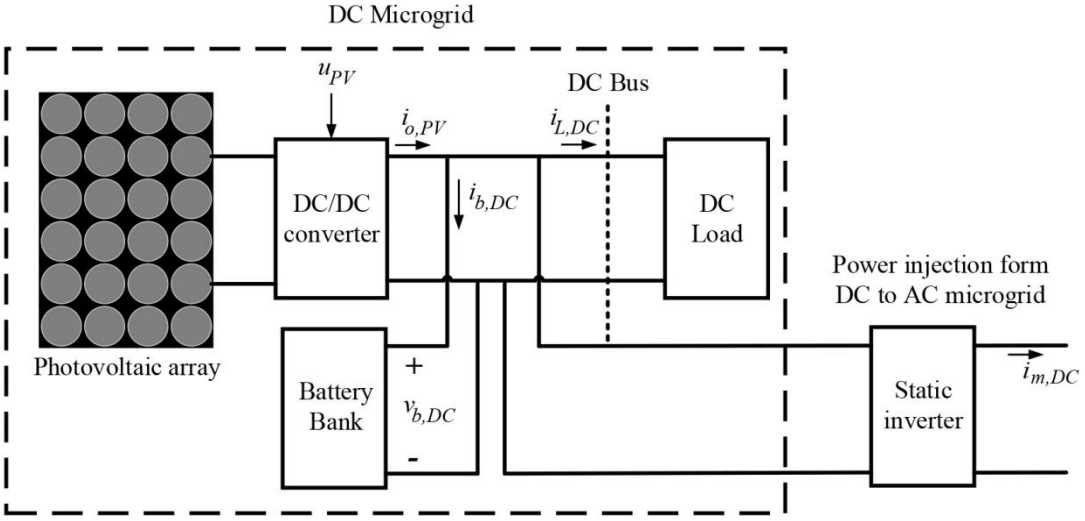

Fig. 3. DC micro-grid scheme

$$i_{PV} = n_p I_{ph} - n_p I_{rs}\left(e^{\frac{qv_{PV}}{n_s BKT}} - 1\right) \quad (11)$$

where n_p represents the number of parallel modules each of which is constituted by n_s cells connected in series, I_{ph} is generated current under a given insolation, I_{rs} is the cell reverse saturation current, q is the charge of an electron, v_{PV} is the output voltage of PV array, B considers the cell deviation from the ideal p-n junction characteristic, K is Boltzmann's constant, and T is the cell temperature.

Also, I_{ph} and I_{rs} can be calculated as follows:

$$\begin{aligned} I_{ph} &= [I_{scr} + K_i(T - T_r)]\frac{\gamma}{100} \\ I_{rs} &= I_{rr}\left[\frac{T}{T_r}\right]^3 e^{\frac{qE_G}{KT}\left[\frac{1}{T_r} - \frac{1}{T}\right]} \end{aligned} \quad (12)$$

where I_{scr} is the cell short-circuit current at reference temperature and radiation, K_i is the short circuit current temperature coefficient, γ is the solar radiation, T_r is the cell reference temperature, I_{rr} is the reverse saturation current at T_r, and E_G is the band-gap energy of the semiconductor used in the cell.

Similar to the AC micro-grid, the DC bus delivers the energy generated by solar subsystem to the DC load as well as battery bank. Also, the DC bus voltage ($v_{b,DC}$) is imposed by the battery bank connected to it. Assuming that the battery bank is modeled as a voltage source $E_{b,DC}$ connected in series with a resistance $R_{b,DC}$ and a capacitance $C_{b,DC}$, the dynamic model of the DC micro-grid may be written as [21]:

$$\begin{cases} \frac{dv_{PV}}{dt} = \frac{i_{PV}}{C} - \frac{i_{o,PV}}{C}u_{PV} \\ \frac{di_{o,PV}}{dt} = -\frac{v_{b,DC}}{L} + \frac{v_{PV}}{L}u_{PV} \\ \frac{dv_{v,DC}}{dt} = \frac{1}{C_{b,DC}}\left(i_{o,PV} - i_{L,DC}\right) \end{cases} \quad (13)$$

where $i_{o,PV}$ is the current on the output terminals of the DC/DC converter, C and L are electrical parameters of the DC/DC converter, u_{PV} is the duty cycle of the DC/DC converter which is used as the control signal, $v_{c,DC}$ is the voltage on $C_{b,DC}$, and $i_{L,DC}$ is the DC load current. Thus, $v_{b,DC}$ can also be calculated through the following equation:

$$v_{b,DC} = E_{b,DC} + v_{c,DC} + \left(i_{o,PV} - i_{L,DC}\right)R_{b,DC} \quad (14)$$

The current $i_{m,DC}$ shown in Fig. 3 corresponds to the power injected from the DC micro-grid to the AC micro-grid.

4. Proposed Load Shedding Scheme

As stated above, the hybrid AC/DC micro-grid can be either connected to the utility grid or disconnected from it. In the first case, an imbalance between the power supplied by the sources and the power demanded by the loads can be solved by trading the power with the utility grid, while in the second case, the renewable power sources are responsible to solve the imbalance. Since in the isolated case, the renewable sources may not be able to supply the whole power demand, the loads are further classified as critical and non-critical loads. The critical loads are the ones which should be supplied in any condition, while the non-critical loads are the ones which are supplied when the generated power is adequate.

In the case of power shortage, load shedding is used to meet the balance, *i.e.* reducing the amount of non-critical loads intentionally while the critical loads are supplied without any interrupt. According to the competing and conflicting claims of consumers for their loads, load shedding by the order of low priority from the view-point of the load importance is not effective. Thus, an effective load shedding scheme is required in micro-grid operation [22] and [23]. Since the load shedding problem is related to distributing insufficient power to consumers requiring more power, it can be considered as a bankruptcy problem [24]-[26]. The bankruptcy problem deals with the problem of how to divide insufficient estate among all claimants. In 1985, Aumann and Maschler have shown mathematically, and through a game theoretic analysis, that assuming an estate of size e, and debts to the creditors 1 and 2, of d_1 and d_2, the Contested Garment Rule linearly interpolates between Equal Division of Gains for $e \leq d_1$, and Equal Division of Losses for $d_2 \leq e$[27]. In this paper, we use the rule extended by Aumann and Maschler to solve the load shedding problem as a bankruptcy problem.

5. Proposed Supervisory Controller

Here, supervisory control for the hybrid AC/DC micro-grid is considered. The operation procedure of the supervisory controller is shown in Fig. 4. As seen in this figure, the supervisory controller first detect whether the micro-grid is operating in grid-connected mode or grid-disconnected mode. For $I_s = 1$, *i.e.* grid-connected mode, the generation systems are set in the maximum power operating point. Also, the state of charge (SOC) of battery banks are checked, where SOC can be calculated as $SOC_k = (\int_0^t i_{b,k}(\tau)d\tau)/(Q_{c,k}^{max})$, where $Q_{c,k}^{max}, k = \{AC, DC\}$are the maximum capacity of the battery bank k, and $i_{b,k}$ is the current across battery bank k. If $SOC_k < 1$, or equivalently the battery bank k is not full, the supervisory controller sets the battery k in the charging mode. It is worth noting that in this case, the charge current is assumed $10\,A$. After checking the SOC of the

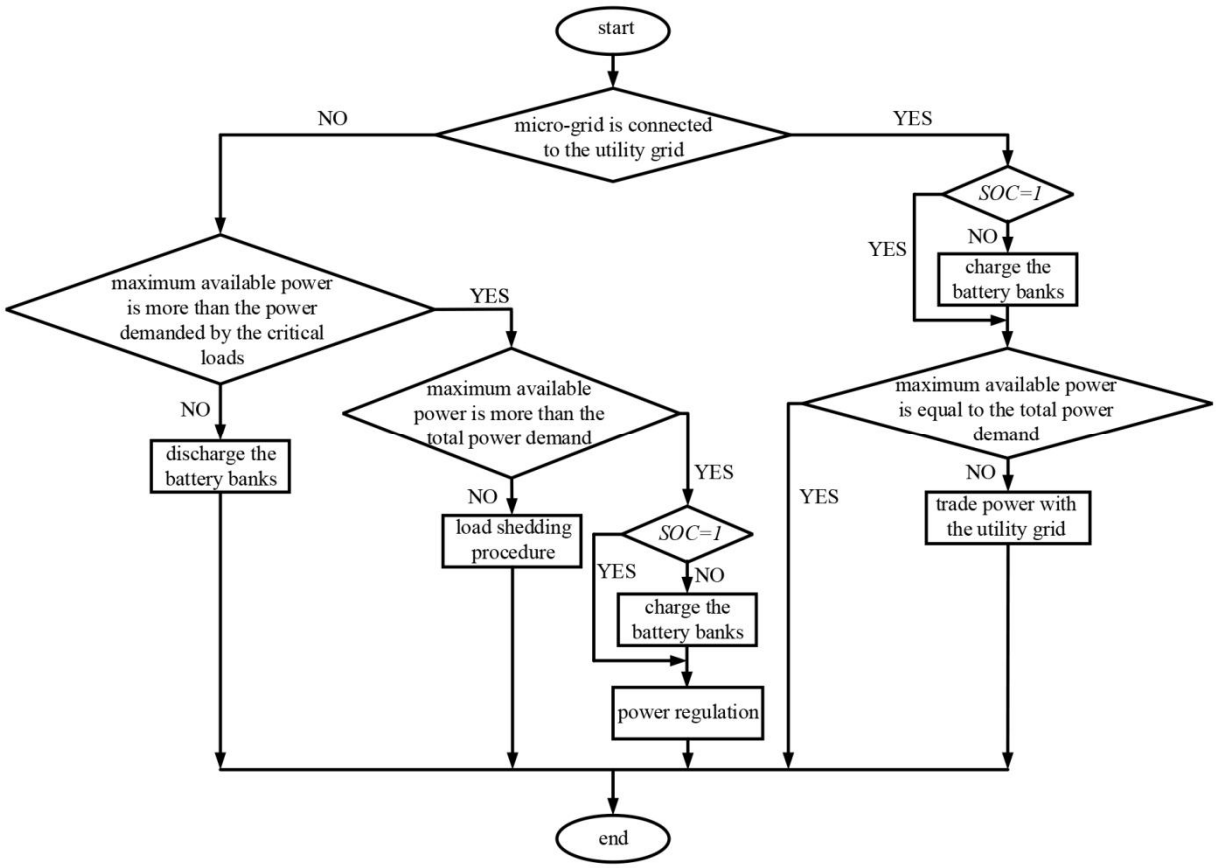

Fig. 4. **The operation procedure of the supervisory controller**

battery banks, maximum available power is calculated and compared to the total power demand. Thus, the supervisor commands the power surplus in the hybrid AC/DC micro-grid to be sent to the utility grid, and power shortage to be supplied by the utility grid. It should be remarked that the main converter acts as a rectifier, or as a static inverter based on the imbalance condition between the AC and DC micro-grids.

For $I_s = 0$, as seen in Fig. 4, the battery banks are only used for supplying the power to the critical loads, *i.e.*, for the case that maximum available power is smaller than the power demanded by the critical loads, the battery banks are set in the discharging mode. Otherwise, the battery banks are remained charged for the possible future power shortage of critical loads. Also, when the maximum available power is more than the total power demand, the SOC of battery banks is checked for possible charge action. Then, the generation systems have to track the total power demand. Load shedding scheme is used when the maximum available power is smaller than the total power demand. In this case, the generation systems can only supply some percentage of the power demanded by the non-critical loads.

As previously mentioned, the wind subsystem acts to either satisfy power demand or track the wind turbine maximum power conversion. To control the wind subsystem, the sliding controller is used, which is in the following form:

$$\begin{cases} if\ p_{WG,max} \geq p_{WG,ref} \Rightarrow u_{WG} = u_I \\ if\ p_{WG,max} < p_{WG,ref} \Rightarrow u_{WG} = u_{II} \end{cases} \quad (15)$$

where u_I, u_{II}can be calculated as given in [28], and the sliding surfaces are

$$\begin{aligned} h_{1,WG} &= p_{WG,ref} - \frac{3}{2}\phi_m i_q \omega_e + \frac{3}{2}\left(i_q^2 + i_d^2\right)R_s \\ h_{2,WG} &= p_{WG,max} - \frac{3}{2}\phi_m i_q \omega_e \end{aligned} \quad (16)$$

where $p_{WG,ref}$ is the demand power reference, involving the load current and the AC battery charge current.

The solar subsystem is also to either satisfy power demand or track the PV array maximum power conversion. It is important to remark that the solar cell voltage corresponding to maximum PV array power ($v_{PV,max}$) may be calculated through

$$\frac{\partial p_{PV}}{\partial v_{PV}} = 0 \quad (17)$$

and the current corresponding to the maximum PV array power ($i_{PV,max}$) can be obtained by Equation (11) by

having$v_{PV,max}$. In this paper, the sliding controller presented in [21] is used to force the solar generation system to track the reference power. The control law can be expressed as given in (18), where the sliding surfaces are

$$\begin{cases} if\ p_{PV,max} \geq p_{PV,ref} \Rightarrow u_{PV} = \begin{cases} 1, if\ h_{1,PV} \geq 0 \\ 0, if\ h_{1,PV} < 0 \end{cases} \\ if\ p_{PV,max} < p_{PV,ref} \Rightarrow u_{PV} = \begin{cases} 1, if\ h_{2,PV} \geq 0 \\ 0, if\ h_{2,PV} < 0 \end{cases} \end{cases} \quad (18)$$

$$h_{1,PV} = \left(i_{L,DC} + I_{b,ref,DC} - i_{o,PV}\right) = 0,\ h_{2,PV} = p_{PV,max} - i_{o,PV} v_{b,DC} = 0 \quad (19)$$

6. SIMULATION RESULTS

In this section, an example is simulated to assess the performance of the proposed supervisory controller, and to demonstrate its effectiveness. Hence, the main converter is assumed to be ideal, *i.e.*, it acts as an ideal rectifier, or as an ideal static inverter. Also, the parameters used in the simulation are also given in Table 1.

TABLE 1. PARAMETERS USED IN SIMULATIONS

Parameter	*Value*	*Parameter*	*Value*
ρ	$1.255\ \left(\frac{Kg}{m^3}\right)$	A	$10.6362\ (m^2)$
r	$1.84\ (m)$	R_s	$0.3676\ (\Omega)$
L	$3.55\ (mH)$	ϕ_m	$0.2876\ (Wb)$
P	28	$E_{b,AC}, E_{b,DC}$	$48\ (V)$
$R_{b,AC}, R_{b,DC}$	$14\ (m\Omega)$	$C_{b,AC}, C_{b,DC}$	$180000\ (F)$
λ_{opt}	8.1	I_{scr}	$3.27\ (A)$
K_i	$0.0017\ \left(\frac{A}{^\circ C}\right)$	J	$7.856\ (Kg.m^2)$
I_{rr}	$2.079 \times 10^{-6}\ (A)$	T_r	$301.18\ (K)$
E_G	$1.1\ (V)$	K	$1.380 \times 10^{-23}\ \left(\frac{Nm}{K}\right)$
n_p	5	n_s	200
q	$1.6 \times 10^{-19}\ (C)$	B	1.6
$Q_{c,AC}^{max}$	$80\ (A.h)$	$Q_{c,DC}^{max}$	$80\ (A.h)$

Assuming that disconnection from the utility grid happens at t=8 (sec), the simulation results are presented in Fig. 5-8. Fig. 5 shows the power exchange between the hybrid AC/DC micro-grid and the utility grid (P_grid), where positive and negative value correspond to power surplus and power shortage condition, respectively. The power injected from the DC micro-grid to the AC micro-grid (P_(inj,AC)) and the power injected form the AC micro-grid to the DC micro-grid (P_(inj,DC))are presented in Fig. 6. The time behavior of the AC micro-grid is presented in Fig. 7, including wind speed (v), power demanded by critical loads $\left(P_{L,AC,C}\right)$, power demanded by non-critical loads $\left(P_{L,AC,NC}\right)$, and the allocated power to the AC non-critical loads (LS), power generated by the wind subsystem (P_{WG}), the state of charge of the battery bank (SOC_{AC}), and power profile of the battery bank $\left(P_{Batt,AC}\right)$. Also, the time behavior of the DC micro-grid is shown in Fig. 8, including cell temperature (T), solar radiation (γ), power demanded by critical loads $\left(P_{L,DC,C}\right)$, power demanded by non-critical loads $\left(P_{L,DC,NC}\right)$, and the allocated power to the DC non-critical loads $\left(P_{L,DC,LS}\right)$, power generated by the solar subsystem (P_{PV}), the state of charge of the battery bank (SOC_{DC}), and power profile of the battery bank $\left(P_{Batt,DC}\right)$. It should be remarked that the steps in the power demand profile refer to abrupt load connection or disconnection. Furthermore, positive and negative value of battery banks power correspond to charge and discharge condition, respectively.

As stated above, for $t \in [0,8](sec)$, the hybrid AC/DC micro-grid is connected to the utility grid. Fig. 5 indicates that for $t \in [5.2,6]\ (sec)$, the micro-grid injects power to the utility grid, while for $t \in [0,5.2]\ (sec)$ and $t \in [6,8]\ (sec)$ power shortage in the micro-grid is supplied by the utility grid. Also, it can be seen in Fig. 6 that for $t \in [8,9.3]\ (sec)$, the DC micro-grid injects power to the AC micro-grid. The DC micro-grid receives power from the Ac micro-grid continuously, except for $t \in [8,11]\ (sec)$. From Fig. 7 and 8, it is obvious that for $t \in [8,13]\ (sec)$, the maximum available power is smaller

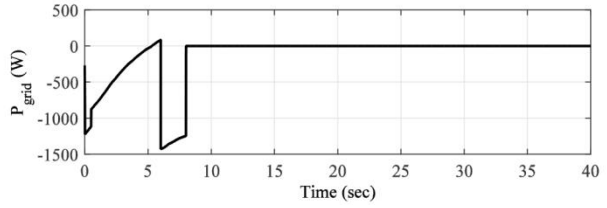

Fig. 5. The power exchange between the hybrid AC/DC micro-grid and the utility grid

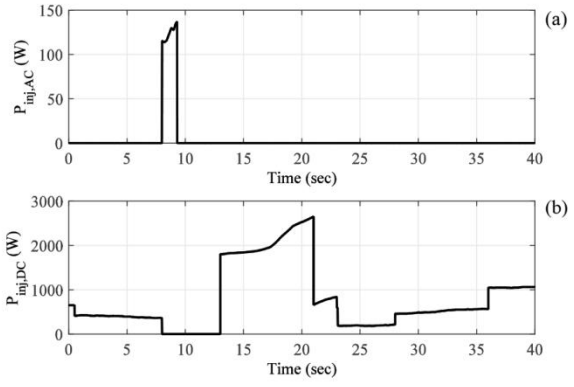

Fig. 6. Power exchange between micro-grids; (a) the power injected from the DC micro-grid to the AC one, (b) the power injected from the AC micro-grid to the DC one

than the power demanded by the critical loads, and consequently the battery banks are set in the discharge mode. Also, for this period of time, the non-critical loads are not supplied. For $t \in [13,21]$, the maximum available power is more than the power demanded by the critical loads, and smaller than the total power demand. Thus, load shedding scheme is applied for this period of time. It is worth noting that the amount of load to be shed of AC and DC non-critical loads for this period of time is shown in Fig. 9 for 8 intervals of $1\ (sec)$. After $t = 21\ (sec)$, the maximum available power gets more than the total power demand by both critical and non-critical loads. Thus, the battery banks are set in the charging mode, and the supervisory controller enforces the generation systems to track the demanded power.

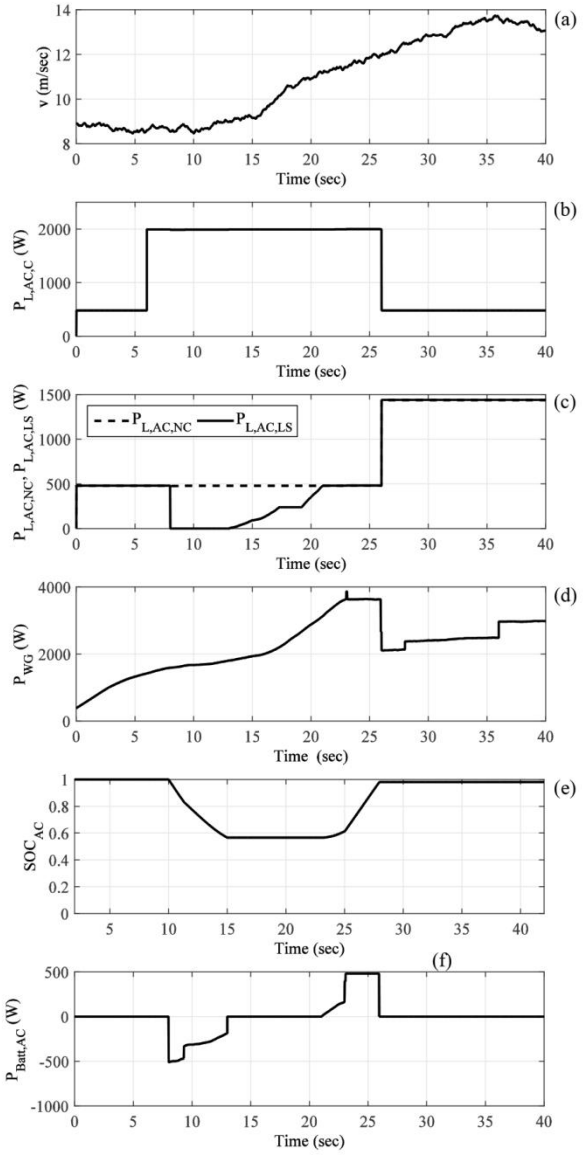

Fig. 7. Time behavior of the AC micro-grid; (a) wind speed (v), (b) power demanded by the critical loads, (c) power demanded by non-critical loads, and allocated power to AC non-critical loads, (d) power generated by the wind subsystem, (e) the state of charge of the battery bank, (f) power profile of the battery bank

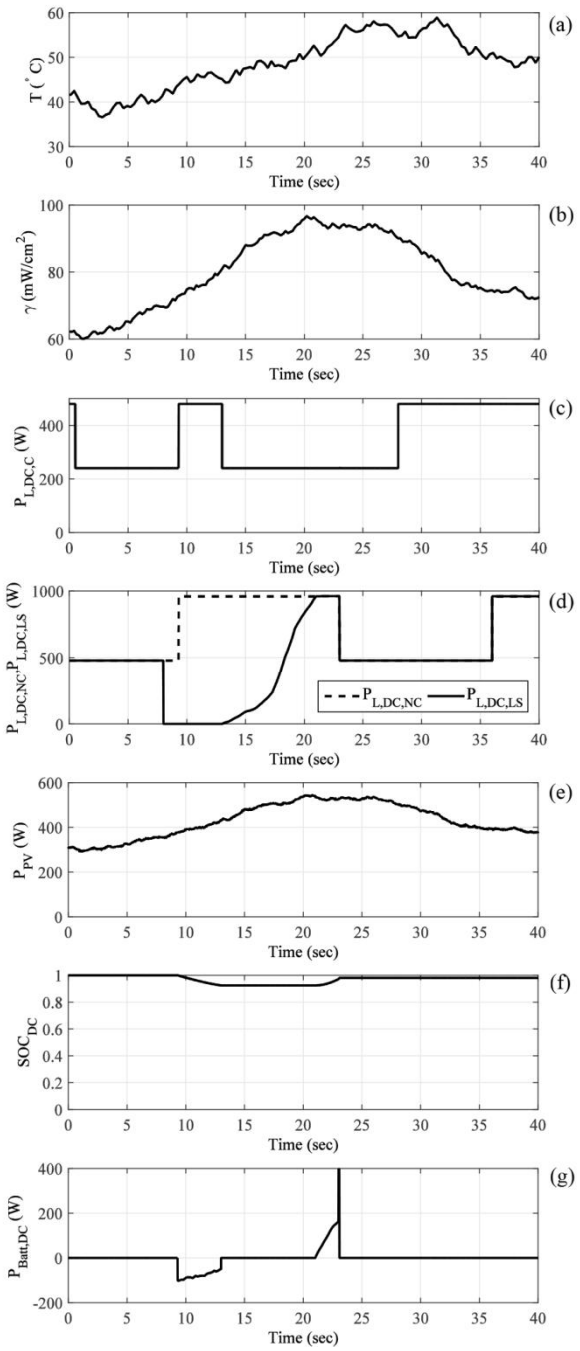

Fig. 8. Time behavior of the DC micro-grid; (a) cell temperature, (b) solar radiation, (c) power demanded by the critical loads, (d) power demanded by non-critical loads, and allocated power to DC non-critical loads, (e) power generated by the solar subsystem , (f) the state of charge of the battery bank, (g) power profile of the battery bank.

The main objective of a power management system is to manage power flow in a micro-grid to satisfy the demanded power. Hence, the performance and the effectiveness of a power management system can be investigated based on the demanded power satisfaction capability. Statistics of the satisfaction of the demanded power by the critical loads are presented in Table 2, where the differences between the generated total power in the

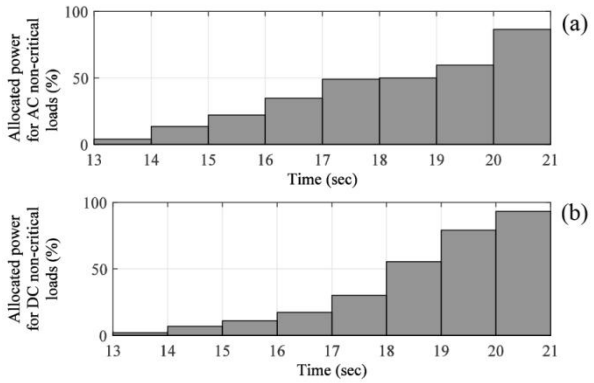

Fig. 9. Amount of the allocated power to non-critical loads (%); (a) allocated power for AC noncritical loads, (b) allocated power for DC noncritical loads

AC micro-grid ($P_{gen,AC}$) and $P_{L,AC,C}$are used as an indicator of the satisfaction of the demanded critical power in the AC micro-grid, and the differences between the generated total power in the DC micro-grid ($P_{gen,DC}$) and $P_{L,DC,C}$are used as an indicator of the satisfaction of the demanded critical power in the DC micro-grid. Furthermore, STD is the standard deviation value of the indicators. As shown in Table 2, the mean value of the not-supplied critical load in the AC micro-grid is 1.4044 (w), and the mean value of the not-supplied critical load in the DC micro-grid is 2.7250 (w), which both values are good and acceptable. Therefore, the proposed supervisory controller has a good performance in satisfying the demanded power by critical loads.

TABLE 2. STATISTICS OF THE INDICATORS OF THE SATISFACTION OF THE DEMANDED POWER BY THE CRITICAL LOADS

Micro-grid	*Indicator*	*Mean*	*STD*
AC	$P_{gen,AC} - P_{L,Ac,C}$	*1.4044*	±5.8039
DC	$P_{gen,DC} - P_{L,Dc,C}$	*2.7250*	±7.1901

Furthermore, the statistics of the amount of the allocated power to the non-critical loads in both AC and DC micro-grids are presented in Table 3. As seen in this table, the mean value of the amount of the allocated power to the non-critical loads in the AC and DC micro-gridsare 88.5500 % and 88.0750 %, respectively. It should be remarked that both values are acceptable promising; therefore, the proposed load shedding scheme can effectively manage the load shedding problem.

TABLE 3. STATISTICS OF THE AMOUNT OF THE ALLOCATED POWER TO THE NONCRITICAL LOADS

Micro-grid	*Mean*	*STD*
AC	*88.5500 %*	±25.9110 %
DC	*88.0750 %*	±28.2084 %

7. CONCLUSION

In this paper, a supervisory controller for a hybrid AC/DC micro-grid was proposed in such a way to satisfy the load power demand in both the AC and DC micro-grids, for both grid-connected and disconnected mode. When the micro-grid is connected to the utility grid, the power imbalance would be solved through power exchange between the micro-grid and the utility grid. Since the generation systems may not be able to supply the whole power demand, the loads are further classified into critical and non-critical loads. In this case, some amount of non-critical loads are reduced to meet the power balance, which is called load shedding. In this paper, load shedding procedure is utilized based on the bankruptcy problem, and the insufficient power is distributed to consumers requiring more power. The resulting performance was evaluated through the study of an example. Simulation results established effectiveness of the proposed supervisor controller.

REFERENCE

[1] P. Wang, L. Geol, X. Liu and F. H. Choo, "Harmonizing AC and DC: A Hybrid AC/DC Future Grid Solution," IEEE Power & Energy Magazine, Vol. 11, No. 3, pp. 76-83, 2013.

[2] X. Liu, P. Wang and P. C. Loh, "A hybrid AC/DC micro-grid," in Proceedings of the International Power Electroics. Conference, Singapore, pp. 746–751, 2010.

[3] F. Valenciaga and P. F. Puleston, "Supervisory Control for a Stand-Alone Hybrid Generation System Using Wind and Photovotaic Energy," IEEE Transactions on Energy Conversion, Vol. 20, No. 2, pp. 398-405, 2005.

[4] W. Qi, J. Liu, X. Chen and P. D. Christofides, "Supervisory Predictive Control of Standalone Wind/Solar Energy Generation Systems," IEEE Transactions on Control Systems Technology, Vol. 19, No. 1, pp. 199-207, 2011.

[5] W. Qi, J. Liu and P. D. Christofides, "Distributed Supervisory Predictive Control of Distributed Wind and Solar Energy Systems," IEEE Transactions on Control Systems Technology, Vol. 21, No. 2, pp. 504-512, 2013.

[6] W. Qi, J. Liu and P. D. Christofides, "A distributed control framework for smart grid development: Energy/water system optimal operation and electric grid integration," Journal of Process Control, Vol. 21, pp. 1504-1516, 2011.

[7] W. Qi, J. Liu and P. D. Christofides, "Supervisory Predictive Control for Long-Term Scheduling of an Integrated Wind/Solar Energy Generation and Water Desalination System," IEEE Transactions

on Control Systems Technology, Vol. 20, No. 2, pp. 504-512, 2012.

[8] G. Seenumani, J. Sun and H. Peng, "A Hierarchical Optimal Control Strategy for Power Management of Hybrid Power Systems in All Electric Ships Applications," 49th IEEE Conference on Decision and Control, Hilton Atlanta Hotel, Atlanta, GA, USA, 15-17 December 2010.

[9] G. Seenumani, H. Peng and J. Sun, "A reference governor-based hierarchical control for failure mode power management of hybrid power systems for all-electric ships," Journal of power sources, Vol. 196, pp. 1599-1607, 2011.

[10] G. Seenumani, J. Sun and H. Peng, "Real-Time Power Manaement of Integrated Power Systems in All Electric Ships Leveraging Multi Time Scale Property," IEEE Transactions on Control Systems Technology, Vol. 20, No. 1, pp. 232-240, 2012.

[11] X. Liu, P. Wang and P. C. Loh, "A Hybrid AC/DC Microgrid and Its Coordination Control," IEEE Transactions on Smart Grid, Vol. 2, No. 2, pp. 278-286, 2011.

[12] C. Jin, P. C. Loh, P. Wang, Y. Mi and F. Blaabjerg, "Autonomous Operation of Hybrid AC-DC Microgrids," in Proceedings of IEEE international conference on sustainable energy technologies (ICSET), Kandy Sri Lanka, Dec. 6-9, 2010.

[13] J. M. Guerrero, P. C. Loh, T. L. Lee and M. Chandorkar, "Advanced Control Architectures for Intelligent Microgrids-Part II: Power Quality, Energy Storage, and AC/DC Microgrids," IEEE Transactions on Industrial Electronics, Vol. 60, No. 4, pp. 1263-1270, 2013.

[14] G. Ding, F. Gao, S. Zhang, P. C. Loh and F. Blaabjerg, "Control of hybrid AC/DC microgrid under islanding operational conditions," Journal of Modern Power Systems and Clean Energy, Vol. 2, No. 2, pp. 223-232, 2014.

[15] R. Geiriha and R. Arivalahan, "Power Management and Decentralized Control of Interlinking Converter by Interfacing AC and DC Micro grids," International Journal of Engineering Science and Innovative Technology (IJESIT), Vol. 3, No. 6, pp. 136-146, 2014.

[16] N. Eghtedarpour and E. Farjah, "Power Control and Management in a Hybrid AC/DC Microgrid," IEEE Transactions on Smart Grid, Vol. 5, No. 3, pp. 1494-1505, 2014.

[17] M. Hosseinzadeh and F. Rajaei Salmasi, "Power management of an isolated hybrid AC/DC micro-grid with fuzzy control of battery banks," IET Renewable Power Generation, vol. 9, no. 5, pp. 484-493, 2015.

[18] R. M. Kamel, A. Chaouachi and K. Nagasaka, "Wind power smoothing using fuzzy logic pitch controller and energy capacitor system for improvement micro-grid performance in islanding mode," Energy, Vol. 35, pp. 2119-2129, 2010.

[19] F. Valenciaga, P. F. Puleston, P. E. Battaiotto and R. J. Mantz, "Passivity/sliding mode control of a stand-alone hybrid generation system", IEE Proceedings-Control Theory Applications, Vol. 147, No. 6, pp. 680-686, 2000.

[20] K. H. Hussein, I. Muta, T. Hoshino and M. Osakada, "Maximum photovoltaic power tracking: an algorithm for rapidly changing atmospheric conditions," IEE Proceedings Generation, Transmission and Distribution, Vol. 142, No. 1, pp. 59-64, 1995.

[21] F. Valenciaga, P. F. Puleston and P. E. Battaiotto, "Power control of a photovoltaic array in a hybrid electric generationn system using sliding mode techniques," IEE Proceedings-Control Theory Applications, Vol. 148, No. 6, pp. 448-455, 2001.

[22] H. M. Kim, T. Kinoshita and Y. Lim, "Talmudic Approach to Load Shedding of Islanded Microgrid Operation Based on Multiagent System," Journal of Electrical Engineering and Technology, Vol. 6, No. 2, pp. 284-292, 2011.

[23] Y. Lim, H. M. Kim and T. Kinoshita, "Distributed Load-Shedding System for Agent-Based Autonomous Microgrid Operations," Energies, Vol. 7, pp. 385-401, 2014.

[24] H. M. Kim, T. Kinoshita and T. H. Kim, "Bankruptcy Problem Approach to Load-Shedding in Agent-Based Microgrid Operation," Security-Enriched Urban Computing and Smart Grid, Vol. 78, pp. 621-628, 2010.

[25] H. M. Kim, T. Kinoshita, Y. Lim and T. H. Kim, "A Bankruptcy Poblem Approach to Load-shedding in Multiagent-based Microgrid Operation," Sensors, Vol. 10, pp. 8888-8898, 2010.

[26] H. M. Kim and T. Kinoshita, "A Comparative Study of Bankruptcy Rules for Load-Shedding Scheme in Agent-Based Microgrid Operation," Ubiquitous Computing and Multimedia Applications, Vol. 151, pp. 145-152, 2011.

[27] R. J. Aumann and M. Maschler, "Game Theoritic Analysis of a Bankruptcy Problem from the Talmud," Journal of Economic Theory, Vol. 36, pp. 195-213, 1985.

[28] F. Valenciaga, P. F. Puleston and P. E. Battaiotto, "Variable structure system control design method based on a differential geometric approach: application to a wind energy conversion subsystem," IEE Proceedings-Control Theory Applications, Vol. 151, No. 1, pp. 6-12, 2004.